

6 **Ajay Kulkarni**  
7 **Semen Kharchenko**  
8 **Rangaramanujam M. Kannan**

## Rheo-optical measurements of the first and third normal stresses of homopolymer poly(vinyl methyl ether) melt

9 Received: 24 August 2005  
10 Accepted: 9 November 2005  
11 © Springer-Verlag 2005

A. Kulkarni · S. Kharchenko ·  
R. M. Kannan (✉)  
Department of Chemical Engineering  
and Materials Science, and Biomedical  
Engineering, Wayne State University,  
5050 Anthony Wayne Drive,  
Detroit, MI 48202, USA  
e-mail: rkannan@chem1.eng.  
wayne.edu  
Tel.: +1-313-5773879  
Fax: +1-313-5773810

R. M. Kannan  
Department of Biomedical  
Engineering, Wayne State University,  
5050 Anthony Wayne Drive,  
Detroit, MI 48202, USA

S. Kharchenko  
Masco R & D,  
Taylor, MI, USA

**Abstract** Normal stresses play a key role in polymer processing, yet accurate measurements are still challenging. Simultaneous rheo-optical measurements are conducted on a poly(vinyl methyl ether) homopolymer melt over a wide range of temperatures and oscillatory shear frequencies, in an effort to measure the normal stresses, by using quantitative flow birefringence measurements. The stress optical rule holds well for this polymer as expected, with the value of the stress optic coefficient of  $(6.38 \pm 0.19) \times 10^{-11} \text{ cm}^2/\text{dyn}$  at  $30^\circ\text{C}$ . The first and third normal stress difference coefficients  $\psi_1^*$ ,  $\psi_3^*$ , calculated using a single memory constitutive equation applied to the stress and birefringence data, are in excellent agreement. The ratio of the measured third and first

normal stress difference coefficients,  $(1-\beta)=0.71 \pm 0.05$ , agrees well with the result of the Doi–Edwards model with independent alignment approximation ( $\beta=0.28$ ). The measurement of normal stress difference coefficients with such small deviations proves the robust nature of the improved rheo-optical instrument and its ability to measure complete stress tensor.

**Keywords** Rheo-optics · Stress optic coefficient · First and third normal stress difference · Poly(vinyl methyl ether)

### 26 Introduction

27 Poly(vinyl methyl ether) (PVME) is a polymer of both  
28 fundamental and practical importance. It is already being used  
29 as a plasticizer in the coating industry, as an adhesive pro-  
30 moter, in lens arrays for optical devices, and in various bio-  
31 medical applications (Polymer Data Handbook 1999; Janusz  
32 2002). The dynamics of a miscible blend of polystyrene/poly  
33 (vinyl methyl ether), which exhibits a lower critical solution  
34 temperature, is extensively studied as a model blend to  
35 understand the effect of blending on the flow, physical, and  
36 thermal properties of polymer blends (Pathak et al. 1999;  
37 Kapnistos et al. 1996). Even though the physical and chemical  
38 properties of pure PVME are well explored, its optical an-  
39 isotropic properties are yet to be investigated in detail (Okano

et al. 1994; Querner et al. 2004; Janik et al. 2003; Neilson  
1962; Spevacek and Hanykova 2002). Monnerie et al. (1985)  
reported some optical measurements (birefringence) while  
performing IR-dichroism experiments on polystyrene/poly  
(vinyl methyl ether) blends, and they speculated that the in-  
herent anisotropy of the molecular unit of PVME might be  
negative due to the ether oxygen, which might result in a  
higher polarizability perpendicular to the chain axis. Simulta-  
neous measurements of stress and birefringence on radically  
cross-linked PVME network in simple elongation to obtain  
the stress optical coefficient were carried out by Muller and  
Stadler (1992).

Simultaneous, quantitative measurements of appropriate  
components of refractive index tensor allow for very sen-  
sitive normal stress measurements through the use of the

12  
13  
14  
15  
16  
17  
18  
19  
20  
21  
22  
23  
24  
25

40  
41  
42  
43  
44  
45  
46  
47  
48  
49  
50  
51  
52  
53  
54

55 stress optical rule (SOR), which states that the stress and  
56 birefringence tensors are proportional and coaxial with  
57 proportionality constant  $C$ .

$$\underline{\underline{\sigma}} = \underline{\underline{n}} / C \quad (1)$$

60 and

$$C = \frac{2\pi}{45} \cdot \frac{(n^2 + 2)^2 \cdot (\alpha_1 - \alpha_2)}{nkT} \quad (2)$$

63 where  $\alpha_1$  and  $\alpha_2$  are the axial and transverse polarizability  
64 of the monomer unit, respectively,  $k$  is the Boltzmann's  
65 constant, and  $T$  is the absolute temperature (Janeschitz-  
66 Kriegl 1983). Equation (2) suggests that molecular basis  
67 for stress optical coefficient originates from the difference  
68 in the polarizability  $\Delta\alpha(\alpha_1 - \alpha_2)$ . According to Flory  
69 (1969), anisotropy in polarizability, i.e.,  $\Delta\alpha$ , is related to  
70 the optical anisotropy parameter,  $\Gamma_2$ , which can be derived  
71 from the rotational isomeric state analysis.

$$\Gamma_2 = \frac{3}{5} \Delta\alpha \quad (3)$$

74 The SOR holds well for a wide range of homopolymers.  
75 However, the optical measurements of the normal stress  
76 rely on the accurate measurements of both the amplitude  
77 and the orientation angle of the appropriate projections of  
78 the birefringence tensor, which facilitate optical measure-  
79 ments of normal stresses using birefringence.

80 The calculated relations then are:

$$n_{12} = 1/2 \Delta n'_{12} \cos(2\chi) \quad (4)$$

81 and

$$n_{11} - n_{22} = \Delta n'_{12} \sin(2\chi), \quad (5)$$

85 where  $\chi$  is the orientation angle of the birefringence and  
86  $\Delta n'_{12}$  is the amplitude of the birefringence in the 1–2 plane  
87 (1, shear; 2, shear gradient; 3, vorticity). Similarly in the 1–  
88 3 plane, the magnitude of the birefringence is  $\Delta n'_{13} =$   
89  $n_{11} - n_{33}$ , since  $\chi=0$  from symmetry.

90 For the case of the oscillatory shear flow, the SOR results  
91 in a relationship between the mechanical stresses ( $\sigma_{12}$ ,  
92 shear stress;  $N_1$  and  $N_3$ , the first and third normal stress  
93 differences, respectively) as follows:

$$\sigma_{12} = 1/(2C) \Delta n'_{12} \cos(2\chi) \quad (6)$$

$$N_1 = 1/C \Delta n'_{12} \sin(2\chi) \quad (7)$$

$$N_3 = 1/C \Delta n'_{13} \quad (8)$$

Measurement of  $N_1$  and  $\sigma_{12}$  by mechanical (Ferry 1980) 100  
and optical (Janeschitz-Kriegl 1983) methods is well- 101  
established. Complete characterization of  $\underline{\underline{\sigma}}$  needs mea- 102  
surement of  $N_2$  or, alternatively,  $N_3=N_1+N_2$ , and this has 103  
been more difficult (Gao et al. 1981; Osaki et al. 1981). 104  
Gao et al. (1981) measured  $N_1$  and  $N_2$  for polystyrene 105  
solutions and found the ratios of these normal stresses to be 106  
about  $-0.22$  to  $-0.25$ . Meissner et al. (1989) successfully 107  
measured the normal stress ratio  $N_2/N_1=0.24$  for low- 108  
density polyethylene melt by use of a custom-built cone 109  
and plate rheometer. Brown et al. (1995) compared optical 110  
and mechanical measurement results for  $N_2$  in step strain 111  
experiments for polystyrene solutions. Magda et al. (1991) 112  
studied the  $N_2$  differences in a liquid crystalline polymer. 113  
The  $N_1$  dependence on shear rate near order–disorder 114  
transition temperature was investigated by Takahashi et al. 115  
(1996). Third normal stress difference ( $N_3$ ) was investi- 116  
gated in melts using mechanical and birefringence mea- 117  
surements by Kannan and Kornfield (1992). In these 118  
studies, they observed  $\beta \sim 0.31$  and  $0.25$  for polyisoprene 119  
(PI) and poly(ethylene–propylene) (PEP) melts, respec- 120  
tively. The effect of temperature, molecular weight, and its 121  
distribution and side-chain branching in  $N_1$  for bulk 122  
homopolymers under shear stress was investigated by 123  
Han and Jhon (1986). Relaxation of  $N_2$  following step 124  
strain for a linear entangled melt of PI was investigated by 125  
Olson et al. (1998). They used a multiple light path tech- 126  
nique to sample the material, and observed  $\beta \sim 0.2-0.24$ , in 127  
between the values predicted with the independent align- 128  
ment approximation (IAA) and without it. In an effort to 129  
fully describe the stress tensor, Van Egmond and 130  
Kalogrianitis (1997) utilized full tensor optical rheometry 131  
technique in which three polarization-modulated beams 132  
were used to probe all independent elements of the refrac- 133  
tive index tensor. Furthermore, the results for the transient 134  
behavior of  $N_2$  and  $-N_2/N_1$  on inception and cessation of 135  
simple shear flow of polystyrene in semidilute solution 136  
were compared with predictions of Doi–Edwards and 137  
Giesekus models. Even though quantitative full stress 138  
tensor measurements were not available, they showed that 139  
the Doi–Edwards model is less successful in predicting 140  
transient results but agrees well with observed steady-state 141  
dependence of  $N_2$  on shear rate. 142

Hence, most of the studies have focused on measure- 143  
ments in solutions, as melts are difficult to deal with due to 144  
the problems with compliance in transducers and the ac- 145  
curate maintenance of temperatures in cone and plate 146  
geometry as changes in density can disturb the gap. Thus, 147  
only little information based on experimental observations 148  
is available describing full stress tensor in oscillatory shear 149  
measurements particularly for homopolymer melts. We 150

151 performed simultaneous measurements of melt rheology  
 152 and flow birefringence. In this paper, we report the stress  
 153 optical coefficient (SOC) for pure PVME melt and after  
 154 slight modification in software processing (which will be  
 155 discussed later in detail), we are able to precisely depict the  
 156 behavior of the first and third normal stress differences  
 157  $\psi_1^*$ ,  $\psi_3^*$  quantitatively, thus describing full stress tensor.

$$\omega^2 \psi_1''(\omega) = G''(\omega) - 1/2G''(2\omega) \quad (13)$$

$$\omega^2 \psi_1^d(\omega) = G'(\omega) \quad (14)$$

## 158 Materials and methods

159 Under small-amplitude oscillatory shear flow, strain, and  
 160 shear stress are described as follows, for the coordinate  
 161 directions described earlier:

- 162 –  $\gamma = \gamma_0 \sin \omega t$ , where  $\gamma_0$  is strain amplitude and  $\omega$  is the  
 163 shear frequency
- 164 –  $\sigma_{12} = \gamma_0(G' \sin \omega t + G'' \cos \omega t)$  where  $G'G''$  is the  
 165 loss modulus

166 Normal stress oscillates with twice the strain frequency  
 167 with a displacement component. In oscillatory shear,  
 168 material functions of normal stresses can be further described  
 169 using complex quantities of the amplitude of normal stress  
 170 coefficients  $\psi_1^*$ ,  $\psi_2^*$  with displacement coefficients  $\psi_1^d$ ,  $\psi_2^d$   
 171 respectively (Ferry 1980):

$$\begin{aligned} N_1 &= \sigma_{11} - \sigma_{22} \\ &= \gamma_0^2 [\omega^2 \psi_1^d + \omega^2 \psi_1' \cos(2\omega t) + \omega^2 \psi_1'' \sin(2\omega t)] \\ N_2 &= \sigma_{22} - \sigma_{33} \\ &= \gamma_0^2 [\omega^2 \psi_2^d + \omega^2 \psi_2' \cos(2\omega t) + \omega^2 \psi_2'' \sin(2\omega t)] \end{aligned} \quad (9)$$

174 where complex amplitudes of normal stresses  $\psi_k^*(\omega)$  are  
 175 defined as:

$$\Psi_k^*(\omega) = \psi_k'(\omega) - i\psi_k''(\omega), k = 1, 2, 3. \quad (10)$$

178 Relationship between material functions of shear stress  
 179 and normal stresses can be sought after substitution of the  
 180 above equations into a particular constitutive equation of a  
 181 single integral memory function (Larson 1988):

$$\sigma = \int_{-\infty}^t M(t-t') [(1-\beta) C^{-1}(t, t') - \beta \cdot C(t, t')] dt \quad (11)$$

184 where  $M(t-t') = \partial G(t-t')/\partial t$  is the memory of linear  
 185 viscoelasticity,  $C^{-1}$  is the Finger tensor,  $C$  is the Cauchy  
 186 tensor, and  $\beta$  is a parameter from 0 to 1.

$$-\omega^2 \psi_1'(\omega) = G'(\omega) - 1/2G'(2\omega) \quad (12)$$

195 Accordingly, it follows that the complex amplitude and  
 196 the displacement coefficient of  $N_3$  are  $\omega^2 \psi_3^*(\omega) = (1-\beta)$   
 197  $\omega^2 \psi_1^*(\omega)$  and  $\omega^2 \psi_3^d(\omega) = (1-\beta)G'(\omega)$ , respectively. The  
 198 validity of this system of equations is verified in previous  
 199 studies (Kannan and Kornfield 1992) and is therefore used  
 200 in our study to confirm the measurements of material  
 201 functions for a simple homopolymer.

## Materials and sample preparation 202

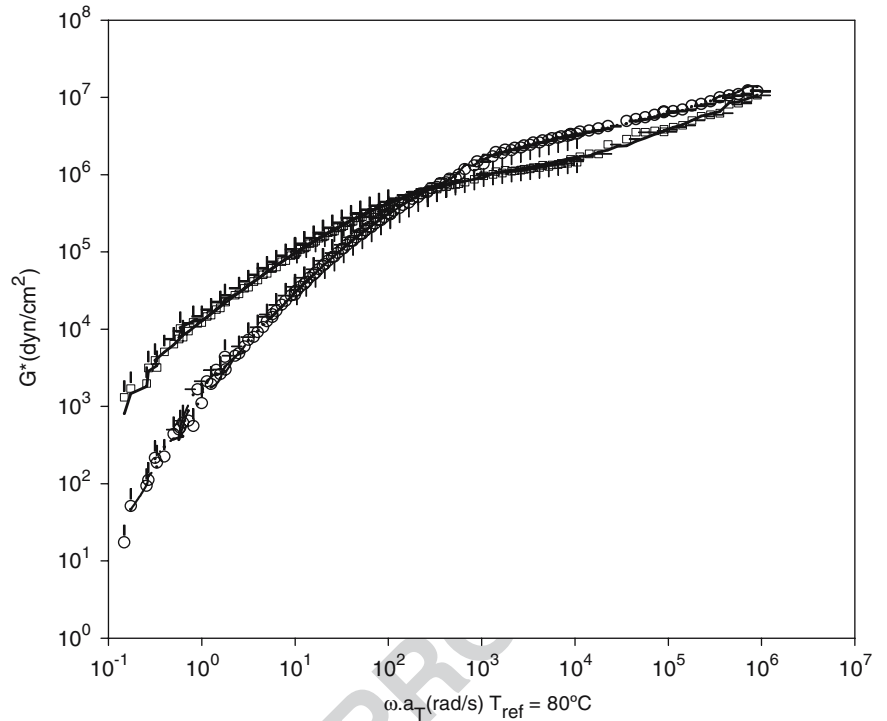
203 PVME was purchased from Scientific Polymer Co. USA  
 204 (MW=90,000 g/mol, PDI=1.5) The PVME was freeze-  
 205 dried to remove water and then purified by dissolving in  
 206 toluene and filtering the solution. The final solution is  
 207 vacuum-dried at room temperature for 3 days and at 80°C  
 208 for 4 days. The removal of solvent was checked by periodic  
 209 weight measurements. The slabs of sample were prepared  
 210 according to the shape of shear sandwich fixture  
 211 (15.1×12.6×1 mm).

## Experimental section 212

213 Simultaneous measurements of stress and flow birefrin-  
 214 gence were performed using a custom-built polarization  
 215 modulation rheo-optical apparatus. The details of the  
 216 apparatus are discussed elsewhere (Johnson et al. 1985;  
 217 Kharchenko et al. 2001). The laser beam is passed through  
 218 the shear–shear gradient plane to obtain shear stress  $\sigma_{12}$   
 219 and complex amplitude of first normal stress difference  
 220 coefficient  $\psi_1^*$ . The complex amplitude of the third normal  
 221 stress difference coefficient ( $\psi_3^*$ ) is obtained by rotating the  
 222 fixture through 90° and passing a laser beam parallel to the  
 223 shear–vorticity plane. The sample was loaded at 80°C and  
 224 excess material was trimmed off along the sides. Small-  
 225 amplitude oscillatory shear experiments were performed  
 226 over the temperature range 0 to +80°C and over a wide  
 227 range of frequencies (100 to 0.01 rad/s) under nitrogen  
 228 atmosphere. The sample was allowed to equilibrate at each  
 229 temperature for 40 min. Dynamic strain sweep experiments  
 230 were conducted to ensure that all applied strains fall in the  
 231 linear viscoelastic region.

232 When using rheo-optical (polarimetric) methods, accu-  
 233 rate measurements of  $N_1$  depend on accurate measurement  
 234 of both the magnitude and the orientation angle of the  
 235 corresponding birefringence component. Because the ratio  
 236 of  $N_1/\sigma_{12}$  scales with strain ( $\gamma$ ), the measurements become

**Fig. 1** Stress optical rule for PVME. Dynamic moduli determined mechanically (*solid line*,  $G'$ ; *dash line*,  $G''$ ) and optically [ $G'_{(opt)}$ ] at different temperatures plotted against shifted frequency. *Circles* represent  $G'_{(opt)}$ , whereas *squares* represent  $G''_{(opt)}$ . (0°C; 30°C; 60°C; 80°C)

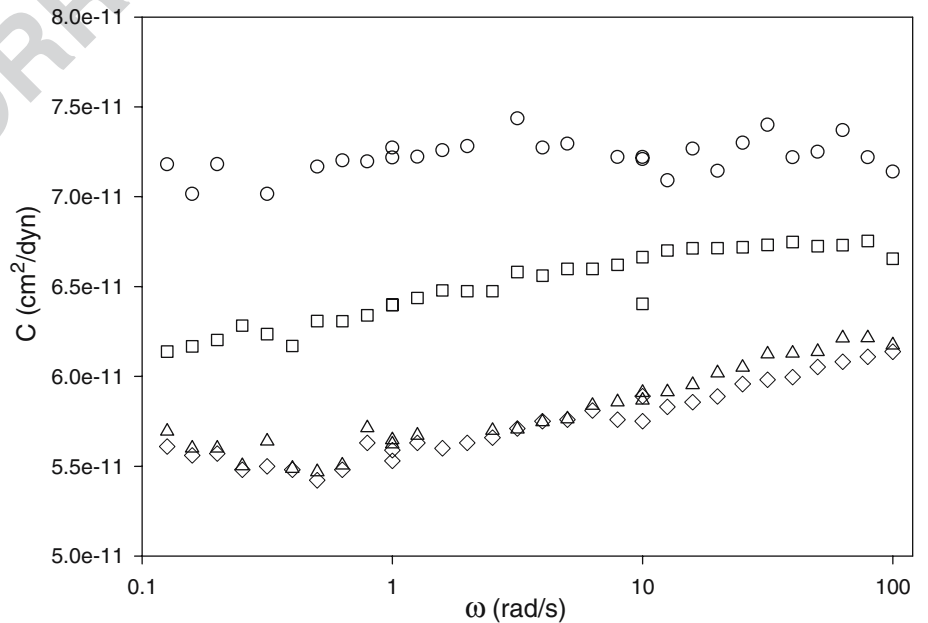


237 a challenge for small strains. This has hampered accurate  
 238 measurements of  $N_1$ , even though the third normal stress  
 239 difference ( $N_3$ ) has been measured with good accuracy  
 240 (Kannan and Kornfield 1992; Osaki et al. 1981). To  
 241 achieve good accuracy in measurements for small  $\gamma$  values,  
 242 we have extensively modified the data acquisition soft-  
 243 ware. In the strain-controlled RSA-II rheometer, the strain

amplitude and the frequency are specified. The applied  
 strain, instead of oscillating about zero, can oscillate about  
 some arbitrary but finite step strain value due to instru-  
 mental limitations. This dc offset in strain results in an  
 additional contribution, since all the measured quantities  
 are proportional to strain. However, the oscillating com-  
 ponents are amplitudes of orientation function, whereas  $\chi$

244  
 245  
 246  
 247  
 248  
 249  
 250

**Fig. 2** Stress optic coefficient  $C$  of PVME homopolymer melt at different temperatures plotted against shifted frequency. Weak temperature dependence was observed consistent with theory. Different *symbols* represent various temperatures. (*Circles*, 0°C; *squares*, 30°C; *triangles*, 60°C; *diamonds*, 80°C)

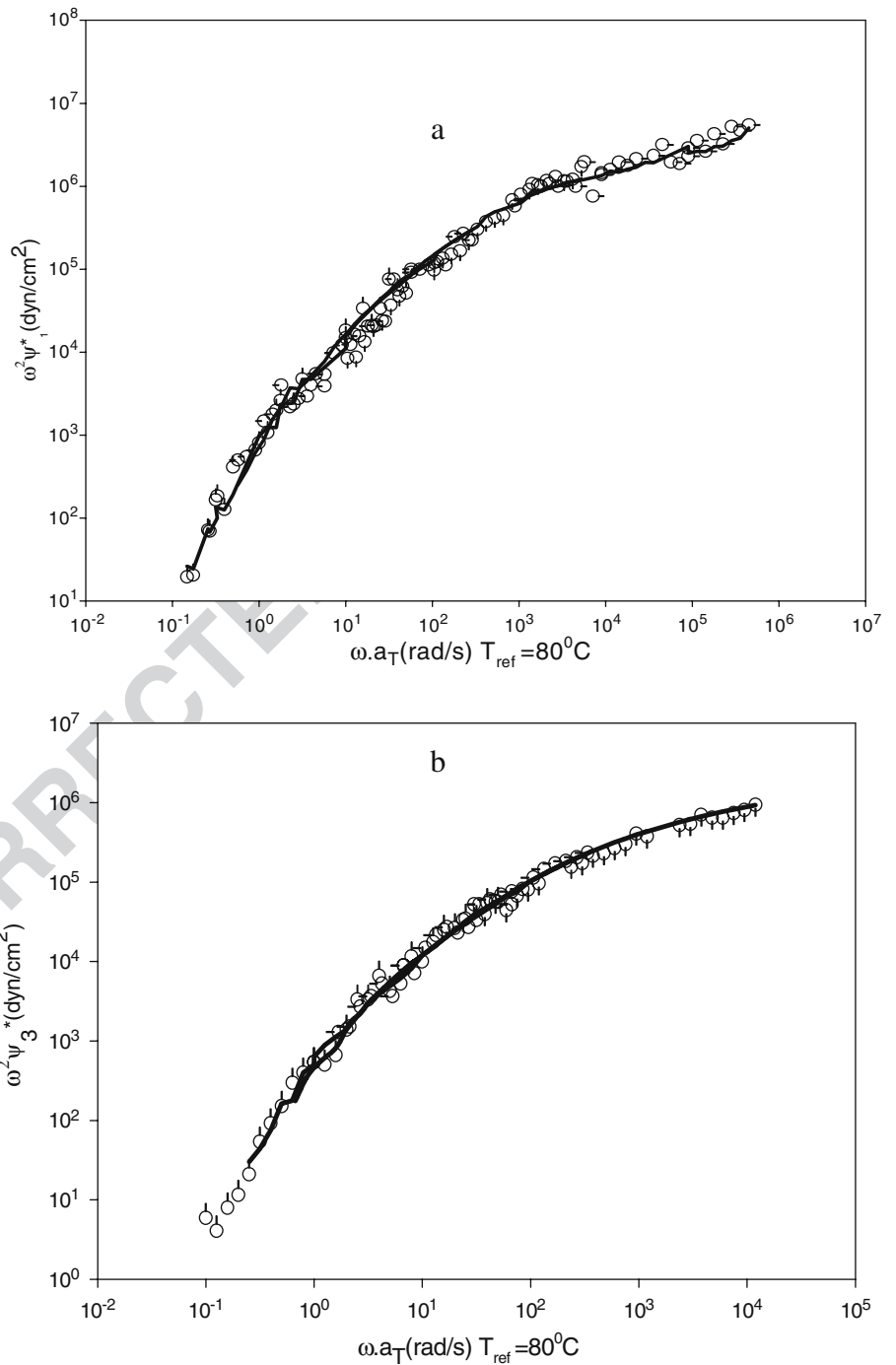


251 is a step function so we take its absolute value. To do this in  
 252 a more accurate manner, we utilize the fact that  $\chi \propto \gamma$ , hence  
 253 the ratio of the contribution to  $\chi$  due to step strain component  
 254 can be determined appropriately, providing us with  
 255 an improved measure of  $\chi$  in the 1–2 plane to enable  $N_1$

measurements. After making modifications in Labview  
 data acquisition software, we were able to measure and  
 analyze the full stress tensor both qualitatively and quan-  
 titatively. The results, to our knowledge, are the first quan-  
 titative measurements of both  $N_1$  and  $N_3$ .

256  
 257  
 258  
 259  
 260

**Fig. 3** **a** Complex amplitude of first and **b** third normal stress difference coefficient calculated mechanically (*solid line*) using Eqs. 13 and 14, and stress optically measured (*symbols*) using Eqs. 7 and 8 plotted against shifted frequency. Temperature distinguished as in Fig. 1



261 **Results and discussion**

## 262 Rheology

263 The master curves for  $G'$  and  $G''$  as a function of shifted  
 264 frequency ( $\omega a_T$ ) are plotted in Fig. 1. Data obtained over  
 265 almost seven decades in reduced frequency cover transition,  
 266 plateau, and terminal region. Time–temperature super-  
 267 position is obeyed. Plateau modulus  $G_N^0$  and entanglement  
 268 molecular weight ( $M_e$ ) of PVME is obtained from these  
 269 data. The value of  $G'$  corresponding to local minimum of  
 270  $\tan \delta$  is taken as plateau modulus.  $G_N^0$  thus calculated has a  
 271 value of 0.402 MPa and compares well with previously  
 272 reported values (Kannan and Lodge 1997). Correspond-  
 273 ingly, the entanglement molecular weight is calculated as,

$$M_e = \frac{\rho RT}{G_N^0} = 6,579 \text{ g/mol} \quad (16)$$

276 where  $\rho$  is the density,  $R$  is the gas constant, and  $T$  is the  
 277 absolute temperature.

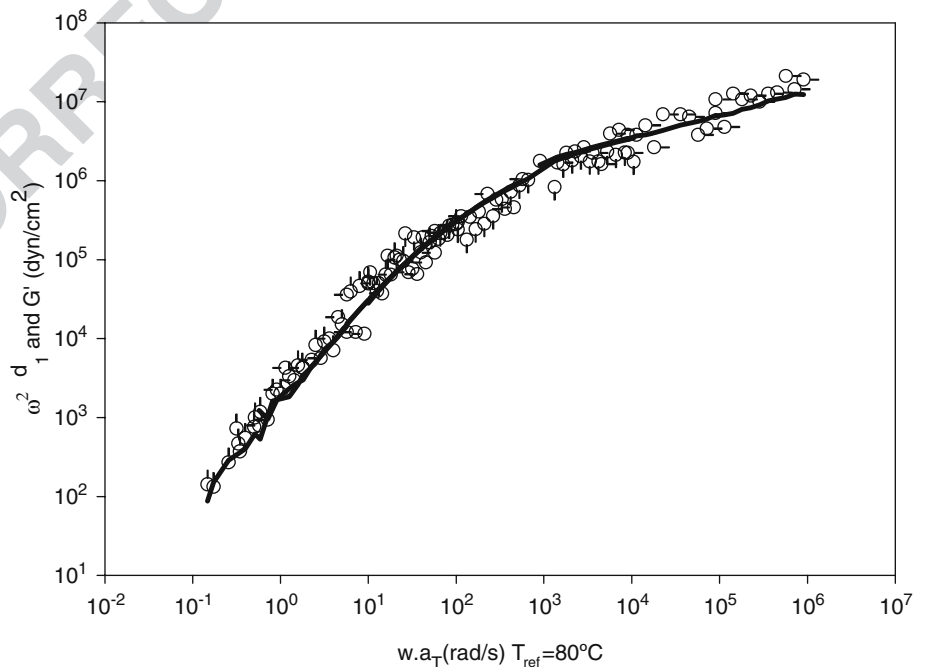
278 Further we calculated tube diameter  $a = b[\rho RT/M_k G_N^0]^{1/2}$   
 279 for the reptation model to be  $a_{\text{PVME}} = 52 \text{ \AA}$ , where  $b = 6.9 \text{ \AA}$  is  
 280 the Kuhn segment length for PVME and  $M_k = 130 \text{ g/mol}$  is  
 281 the molecular weight for this segment. These values agree  
 282 well with values reported in literature (Pathak et al. 1999).

## Flow birefringence

284 The stress optical rule holds over the temperature and  
 285 frequency range used in this study, as evidenced by the fact  
 286 that the dynamic moduli calculated from birefringence data  
 287 superimpose well with the mechanical data (Fig. 1). To our  
 288 knowledge, this is one of the first studies on the flow  
 289 birefringence behavior of pure PVME melt. The value of  
 290 SOC,  $C$ , is reported to be  $(6.38 \pm 0.19) \times 10^{-11} \text{ cm}^2/\text{dyn}$   
 291  $(6.38 \times 10^{-10} \text{ m}^2/\text{N})$  at  $30^\circ\text{C}$ . This value of  $C$  is found to be  
 292 frequency independent. A weak temperature dependence of  
 293 the stress optical coefficient appears to be consistent with  
 294 the theory of entropic elasticity, which predicts that for a  
 295 given amount of conformational distortion (i.e., birefrin-  
 296 gence) an increase in entropic stress is observed with an  
 297 increase in absolute temperature (Fig. 2). For PVME, we  
 298 have sufficient results to compare the temperature depen-  
 299 dence of  $C$  to one linear in reciprocal temperature as  
 300 suggested by the Kuhn–Grun theory (Janeschitz-Kriegl  
 301 1983; Kuhn and Grun 1946). Indeed, our limiting data on  
 302 PVME are described by  $C \times 10^{-11} (\text{cm}^2/\text{dyn}) = 1.0 + \frac{1700}{T}$ ,  
 303 where  $T$  is the absolute temperature (Kelvin).

304 We also calculated the anisotropy of polarizability  $\Delta\alpha$  and  
 305 optical anisotropy parameter  $\Gamma_2$  by using Eqs. 2 and 3,  
 306 respectively, and may be useful in extracting PVME compo-  
 307 nent orientation/relaxation dynamics from blend measure-  
 308 ments. These values are in good agreement with previous  
 309 results on cross-linked PVME (Muller and Stadler 1992).

**Fig. 4** Displacement coefficient of first normal stress difference. Open symbols represent stress optically measured  $\omega^2 \psi_1^d(\omega)$ . Solid curves represent  $Gt$ . Temperature distinguished as in Fig. 1



## 310 Discussion

311 One of the main advantages of using this modified instru-  
 312 mental system is that we can calculate first and third normal  
 313 stress difference coefficients in an accurate manner. With the  
 314 help of constitutive equations, the values of the amplitude of  
 315  $\psi_1^*$  obtained from mechanical data and optical measurements  
 316 agree very well. The ratio of the amplitude of the complex first  
 317 normal stress difference coefficient, measured optically to  
 318 calculated, (i.e.  $|\psi_{1(\text{opt})}^*|/|\psi_{1(\text{cal})}^*|$ ), is reported to be  $0.97 \pm$   
 319  $0.12$  (Fig. 3a). Similarly, the ratio of the third normal stress  
 320 difference coefficient ( $|\psi_{3(\text{opt})}^*|/|\psi_{3(\text{cal})}^*|$ ) is reported to be  
 321  $1.01 \pm 0.09$  (Fig. 3b). Using the equation  $\omega^2 |\psi_3^*(\omega)| =$   
 322  $(1 - \beta)\omega^2 |\psi_1^*(\omega)|$ , we calculated the value of  $\beta$  to be  
 323  $0.29 \pm 0.05$ . The displacement of the first and third normal  
 324 stress difference coefficient ( $\psi_1^d, \psi_3^d$ ) is calculated by  
 325 use of the equations  $\omega^2 \psi_1^d(\omega) = G'(\omega)$  and  $\omega^2 \psi_3^d(\omega) =$   
 326  $(1 - \beta) * G'(\omega)$ . The resulting plot for  $\psi_1^d$  is shown in  
 327 Fig. 4. Similar reasonable agreement between optical and  
 328 mechanical measurements is observed for  $\psi_3^d$  (not shown  
 329 here).

330 Numbers of models predict a nonzero value of  $\beta$  for  
 331 polymer melts. According to the reptation theory (Doi and  
 332 Edwards 1986) for entangled melts in plateau and terminal  
 333 regime,  $\beta$  should be independent of chemical structure of  
 334 polymer. Several attempts have been made to verify this pro-  
 335 position. Kannan and Kornfield (1992) reported  $\beta=0.31$  and  
 336  $0.25$  for PEP and PI, respectively. Osaki et al. (1981) found  
 337  $\beta=0.19$  somewhat lower than expected by the model. This  
 338 was attributed to higher shear rate applied in those studies.

339 The value we obtained for linear, entangled PVME  
 340 ( $\beta=0.29$ ) is in accord with the reptation result with IAA  
 341 ( $0.28$ ) than that without IAA ( $0.14$ ). The modifications in

the data acquisition/analysis protocols allowed for precise  
 measurements of  $N_1$  and  $N_3$ , which further allowed for  
 experimental measurement of  $\beta$ .

## Properties of poly(vinyl methyl ether)

Property	Value	
SOC (cm <sup>2</sup> /dyn)	$(6.38 \pm 0.19) \times 10^{-11}$	347
$\beta$	$0.29 \pm 0.05$	349
$\Delta\alpha$ (10 <sup>25</sup> cm <sup>3</sup> )	13.6	351
$\Gamma_2$ (10 <sup>25</sup> cm <sup>3</sup> )	8.16	354
$G_{N_t}^{0+}$ (MPa)	0.402	355
$M_c^{N_t}$ (g/mol)	6,579	356

†At or relative to the reference temperature of 80°C 360

## 361 Conclusions

362 We have carried out simultaneous, small-amplitude  
 363 oscillatory shear measurements of stress and birefringence  
 364 on PVME homopolymer melt over a wide dynamic range.  
 365 Our results show that the stress optical rule holds for  
 366 PVME with stress optical coefficient,  $C$  (30°C) =  $(6.38 \pm$   
 367  $0.19) \times 10^{-11}$  cm<sup>2</sup>/dyn. Weak temperature dependence of  
 368 SOC was observed as expected by entropic elasticity  
 369 theory. After modifications to the data acquisition and  
 370 analysis software, we were able to provide quantitative,  
 371 accurate optical measurements of the full stress tensor in  
 372 the melt state. Furthermore, the ratio of normal stresses  $\beta$  is  
 373 found to be  $0.29 \pm 0.05$ , which is in good agreement with the  
 374 Doi–Edwards model with IAA) prediction ( $\beta=2/7$ ). 375

376 **Acknowledgement** This work was supported financially by the  
 377 National Science Foundation through DMR grant 9876221 (Institute  
 378 for Manufacturing Research, Wayne State University). 379

## 380 References

- 381  
 382  
 383  
 384 Brown EF, Burghardt WR, Kahvand H, Venerus DC (1995) Comparison of  
 385 optical and mechanical measurements of second normal stress difference relax-  
 386 ation following step strain. *Rheol Acta* 34:221–234  
 387  
 388 Doi M, Edwards SF (1986) The theory of polymer dynamics. Clarendon, Oxford  
 389  
 390 Ferry JD (1980) Viscoelastic properties of polymers, 3rd edn. Wiley, New York  
 391  
 392 Flory PJ (1969) Statistical mechanics of chain molecules. Interscience, New York  
 393  
 394 Gao HW, Ramachandran S, Christiansen EB (1981) Dependency of the steady-state  
 395 and transient viscosity and first and second normal stress difference func-  
 396 tions on molecular weight for linear mono and polydisperse polystyrene  
 397 solutions. *J Rheol* 25:213–235  
 398  
 399  
 400  
 401  
 402  
 403  
 404  
 405  
 406  
 407  
 408  
 409  
 410  
 411  
 412  
 413  
 414  
 415  
 416  
 417  
 418  
 419  
 420  
 421  
 422  
 423  
 424  
 425  
 426  
 427  
 428  
 429  
 430  
 431  
 432  
 433  
 434  
 435  
 436  
 437  
 438  
 439  
 440  
 441  
 442  
 443  
 444  
 445  
 446  
 447  
 448  
 449  
 450  
 451  
 452  
 453  
 454  
 455  
 456  
 457  
 458  
 459  
 460  
 461  
 462  
 463  
 464  
 465  
 466  
 467  
 468  
 469  
 470  
 471  
 472  
 473  
 474

- 422 Kharchenko SB, Kannan RM, Cernohous JJ, Monnerie L, Faivre JP, Jasse B (1985) 447  
423 Venkataramani SS, Babu GN (2001) Orientation and relaxation in uniaxially 448  
424 Unusual contributions of molecular ar- stretched poly(vinyl methyl ether)- 449  
425 chitecture to rheology and flow birefrin- atactic polystyrene blends. *Polymer* 450  
426 gence in hyperbranched polystyrene 26:879  
427 melts. *J Polym Sci B Polym Phys* 39:2562  
428  
429 Kuhn W, Grun F (1946) Statistical behavior of Muller G, Stadler R (1992) Stress-optical 451  
430 of the single chain molecule and its behavior of miscible poly (methyl vinyl 452  
431 relation to the statistical behavior of ether)-cross-polystyrene semi-IPN's 453  
432 assemblies consisting of many chain above glass transition temperature. 454  
433 molecules. *J Polym Sci* 1:193 *Makromol Chem* 202:362  
434 Larson RG (1988) Constitutive equations Okano K, Takada M, Kurita K, Furusaka M 455  
435 for polymeric melts and solutions. (1994) Interaction parameters of poly 456  
436 Butterworths, Boston (vinyl methyl ether) in aqueous solution 457  
437 Magda JJ, Baek SG, Devries KL, Larson RG as determined by small-angle neutron 458  
438 (1991) Shear flows of liquid-crystal scattering. *Polymer* 35(11):2284-2289 459  
439 polymers—measurements of the 2nd Olson DI, Brown EF, Burghardt WR (1998) 460  
440 normal stress difference and the Doi Second normal stress difference relax- 461  
441 molecular theory. *Macromolecules* ation in a linear polymer melt following 462  
442 24:4460-4468 step-strain. *J Polym Sci B Polym* 463  
443 Meissner J, Garbella RW, Hostettler J (1989) Phys 36:2671-2675 464  
444 Measuring normal stress differences in Osaki K, Kimura S, Kurata M (1981) 465  
445 polymer melt shear flow. *J Rheol* 33 Relaxation of shear and normal stresses 466  
446 (6):843 in step-shear deformation of a polysty- 467  
447 rene solution. Comparison with the 468  
448 predictions of the Doi-Edwards theory. 469  
449 *J Polym Sci B Polym Phys* 19:517-527  
450  
451 Pathak JA, Colby RH, Floudas G, Jerome G 452  
453 (1999) Dynamics in miscible blends 453  
454 of polystyrene and poly(vinyl methyl 454  
455 ether). *Macromolecules* 32:2553-2561 455  
456 *Polymer Data Handbook* (1999) Oxford 456  
457 University Press, Oxford, p 956 457  
458 Querner C, Schmidt T, Arndt K (2004) 458  
459 Characterization of structural changes 459  
460 of poly(vinyl methyl ether)  $\gamma$ -irradiated 460  
461 in diluted aqueous solutions. *Langmuir* 461  
462 20(7):2883-2889 462  
463 Spevacek J, Hanykova L (2002) 16th 463  
464 European experimental NMR confer- 464  
465 ence, Prague, June 9-14, 2002 465  
466 Takahashi Y, Noda M, Ochiai N, Noda I 466  
467 (1996) Shear-rate dependence of first 467  
468 normal stress difference of poly(iso- 468  
469 prene-*b*-styrene) in solution near the 469  
470 order-disorder transition temperature. 470  
471 *Polymer* 37:5943-5945 471  
472 Van Egmond JW, Kalogrianitis SG (1997) 472  
473 Full tensor optical rheometry of poly- 473  
474 mer fluids. *J Rheol* 41(2):343-364 474